

RESEARCH ARTICLE

Controlled Delivery of Levothyroxine using a Drug carrier Cu(II) metal-organic framework

Elham Rostami^{1*}, Zeinab Ansari-Asl¹, Elham Hoveizi²

¹ Department of Chemistry, Faculty of Science, Shahid Chamran University of Ahvaz, 67149, Ahvaz, Iran

² Department of Biology, Faculty of Science, Shahid Chamran University of Ahvaz, 67149, Ahvaz, Iran

ARTICLE INFO

Article History:

Received 13 Jan 2024

Accepted 27 Mar 2024

Published 01 Apr 2024

Keywords:

Levothyroxine

Cu(II)-BTC

Drug Delivery

Cell viability

ABSTRACT

Populations suffer from chronic disorders especially hypothyroidism. To decrease thyroid-stimulating hormone (TSH) and medicate hypothyroidism in patients were diagnosed with thyroid cancer and nodular thyroid disease, levothyroxine is utilized clinically. Applications of metal-organic frameworks (MOFs) in various fields of medicine have attracted much attention. Loading levothyroxine onto the nanostructured Cu(II)-MOFs, Cu(II)-BTC, as well as subsequent drug release behavior were studied. Nanostructured Cu(II)-BTC was used to load and release the drug levothyroxine. The obtained results confirmed that besides effects regarding the stability and release of the levothyroxine in phosphate buffer solution (pH=7.4, 10 mM), surface characteristics would affect compounds affinity towards particles. The morphology investigation of the surface roughness was characterized by SEM and AFM. Drug loading amount was determined by Thermal Gravimetric Analysis (TGA). The drug release profiles are characterized by UV spectrophotometry in phosphate buffer solution (PBS), which confirms that they are released in their active form. The release of levothyroxine was studied by detecting in 7 days. The concentration of levothyroxine increased; it was achieved to normal limitation ($12.5 \mu\text{g mL}^{-1}$). Based on the results, $10 \mu\text{M}$ concentration of levothyroxine was determined within 24 h as IC50 concentration in WJMSCs. A comparison of levothyroxine and loading levothyroxine showed that the amount of levothyroxine cytotoxicity was significantly higher than loading levothyroxine ($P < 0.05$). Also, there were significant morphological changes such as shrinkage in treated cells with levothyroxine than loading levothyroxine.

How to cite this article

Rostami E., Ansari-Asl Z., Hoveizi E. Controlled Delivery of Levothyroxine using a Drug carrier Cu(II) metal-organic framework. *Nanomed Res J*, 2024; 9(1): 38-51. DOI: 10.22034/nmrj.2024.01.005

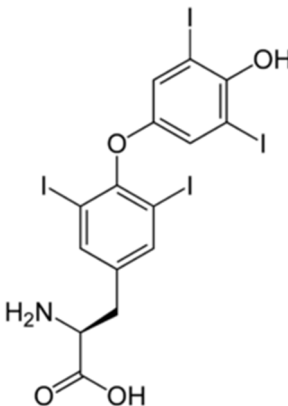
INTRODUCTION

Nowadays, porous structures owing to their various potential applications in biomedicine fields including tissue engineering, drug delivery, and wound healing are tremendously investigated [1-3]. Metal-organic frameworks (MOFs) are a category of porous solids that are fabricated from various metal ions or metal cluster ions with organic linkers. These materials have promising properties including highly tuneable composition, biodegradability, and adequate biocompatibility [4, 5]. Using MOFs as drug carriers has been investigated by many research groups. For example, Lu L *et al.* loaded ibuprofen into the UiO-66-NH₂@

Polysilsesquioxane nanocomposites and reported high capacity of loading and promising release properties of the as-prepared nanocomposites [6]. Orellana-Tavra C *et al.* synthesized a Bismuth-MOF, CAU-7, as a carrier for loading and delivery α -CHC (α -cyano-4-hydroxycinnamic acid) and DCA (sodium dichloroacetate) anticancer drugs, and reported 9 and 33 wt.% for α -CHC and DCA loading contents, respectively [7]. To overcome some limitations of 5-fluorouracil (5-FU) anticancer drug such as off-target distribution, limited half-life, and serious side effects, Liu W *et al.* reported the 5-FU loading into a water-stable Cu(II)-MOF [8]. According to the literature, Fe(III) and Cu(II) MOFs containing carboxylate ligands

* Corresponding Author Email: e.rostami@scu.ac.ir

Table 1. Characteristics of Levothyroxine

Drug	Structure	Mw (g/mol)	Melting point (°C)	Molecular formula
Levothyroxine		776.87 g.mol ⁻¹	231–233 °C	C ₁₅ H ₁₁ I ₄ NO ₄

had suitable characteristics for application in drug delivery systems [9, 10].

Nonspecific distribution of drug throughout the body that causes to rapid clearance, high doses, and poor pharmacokinetics is considered as a limitation of recent drug therapeutics [11-12]. Among different ways to enhance the efficiency of conventional drugs, therapeutics based on nanoparticles have attracted much attention over the past years. These new systems can eliminate some problems of small-molecule drugs. Generally, a nontherapeutic is constructed from an active agent attached to a carrier such as micelles, polymeric nanoparticles, iron oxide, or liposomes [13]. For drug delivery and biomedical applications, the nanoparticles' cytotoxicity is particularly important and strongly affect different aspects of the metabolism in the body. The properties and cytotoxic effects of particles depend strongly on the surface chemistry, sized, and charge of particles [9].

Carrier loading yield depends on the characteristic of both the nanostructure and the loaded substances in addition to the loading solutions. Drug delivery systems should improve the bioavailability of weakly absorbed drugs, while decreasing their effective dose [14, 15]. These properties also influence the drug release of the particles and potentially the carrier stability of the supporting matrix [16].

Levothyroxine is used clinically to treat hypothyroidism and to suppress thyroid-stimulating hormone (TSH) secretion in patients with nodular thyroid disease or thyroid cancer and

thyroid neoplasia. The narrow therapeutic index of this drug demands personalized dosage titration for each patient in order to achieve the necessary therapeutic effect while minimizing toxicity. Overdose is not innocuous, potentially resulting in bone loss as well as changes in cardiac and hepatic function [16-19]

The T₄ hormone is mainly bound to thyroxine-binding Globulin (TBG), reversibly [18]. The growth and development, carbohydrate metabolism, lipid, and proteins are affected by thyroid hormones [17-19].

For elderly person who has cardiac disease or severe hypothyroidism, administrations of levothyroxine products in the range of 12.5-25 µg is recommended; until patients with primary hypothyroidism be clinically euthyroid and the serum TSH has reached normal levels. The American Association of Clinical Endocrinologists and the American Thyroid Association have guidelines to achieve the suitable clinical outcome [17-19].

In general, levothyroxine therapy should be established at full replacement doses early. Physical growth and intellectual development of children can be endangered due to delay in the diagnosis and treatment [20]. Delivery of levothyroxine through oral and transdermal routes for subcutaneous lipid digestion has been reported [21, 22]. Recently, the potential of solid lipid nanoparticles (SLN) [23], the PEG-modified SLN [24], and chitosan [25] for levothyroxine delivery has been investigated. The obtained results exhibited higher drug

loading capacities and sustained release of drug under physiological situations for up to seven days. Thyroid experts establish that levothyroxine materials would not cause to a similar therapeutic results, especially for patients that tight control was necessary (for example, elderly patients with cardiac disease, new-borns, and patients with thyroid cancer) [16, 26]. Endogenously produced T_4 and exogenous levothyroxine are not physiologically and biochemically distinguishable. The advantages of Cu(II)-BTC are considerable although this field of study is new and most of toxicity investigations have mainly conducted for implant applications [27-28].

According to the obtained data, the drug delivery by Cu(II)-BTC and its enhanced drug-loading capacity is investigated using levothyroxine. MOFs owing to their suitable pore size and high surface area are potential candidates for drug delivery objectives. These unique characteristics of MOFs are best suited for different applications such as drug encapsulation and versatile functionality for post synthetic grafting of drug molecules. In comparison to conventional drug delivery ways consisting of oral, rectal, buccal, intramuscular, and intravenous, MOFs have a high potential for drug-loading and better controlled release kinetics [10,18-20].

The main goal of present work is that the loading and release of levothyroxine in Cu(II)-BTC were studied using UV spectrophotometry for seven days. The effect of chemical structure of Cu(II)-BTC, specific surface area, was also investigated on the absorption of levothyroxine and increasing stability and the dissolution of the poorly soluble drugs. The general objective of this study is to design and use a levothyroxine new nano-carrier.

MATERIALS AND METHODS

Materials

The drug, levothyroxine sodium 100%, was provided by Iran Hormone Company. The solvents utilized in the loading experiments, i.e., ethanol, dimethyl sulfoxide (DMSO) 99.5%, sodium dihydrogen phosphate 2-hydrate reagent $NaH_2PO_4 \cdot 2H_2O$ 99% and disodium hydrogen orthophosphate do dehydrate $Na_2HPO_4 \cdot 12H_2O$ 99% were purchased from Sigma Aldrich (HPLC grade). All chemicals were utilized as be awarded. Copper(II) nitrate trihydrate 97 %, was obtained from Merck company.

Human wharton's jelly mesenchymal stem cells (WJMSCs) were cultured in DMEM (Gibco, USA) media supplemented with 1% penicillin/streptomycin (Gibco, USA) and 12% FBS (Gibco, USA). WJMSCs were incubated at 37 °C with 5% CO₂ in a tissue culture flask (SPL, Korea) until the third passage. Then the cells were passaged by trypsin (Gibco,USA), as the confluence was 70-80%. Also, morphology changes in treated and control groups were observed by an inverted microscope (bioered, USA).

The cell survival percentage was quantitatively measured by MTT (3-(4,5-Dimethyl-2-thiazolyl)-2,5-diphenyl-2H-tetrazolium bromide, Sigma, USA, 98%) assay. Briefly, the WJMSCs were cultured in 1×10^4 cell/well in 96-well plate and treated with 25, 10, 5, 1, and 0.5 μ M concentrations of drugs for 24 h then the cells washed with PBS and exposed with 0.5 mg/ml concentration of MTT solution for 4 h. The resulting formazan was dissolved in DMSO (100 ml/well) and the absorbance was calculated at 570 nm by using an ELISA reader (Fax stat, USA). In this study, the concentrations 1000, 500, 100, 10, and 1 μ g/ml of Cu-BTC were used and the untreated cells were determined as a control group. AO/EB staining was done to verify the cell viability. Briefly, the cells were cultured in a 96 well plate and treated with the 10 μ M concentration of Levothyroxine and Cu-BTC loaded by levothyroxine for 24 h. The untreated cells were considered as the control group. The samples were rinsed with PBS and stained with AO/EB (1:1, Sigma,USA) solution for 10 min, then the cells were washed with PBS and observed under a fluorescent microscope (Olympus, Japan).

Synthesis of Cu-BTC

The Cu-BTC as a porous MOF was prepared through the mixing of 0.5 g (2.38 mmol) of trimesic acid in 100 mL of H₂O: DMF: EtOH with a solution of 1.05 g (4.34 mmol) of Cu(NO₃)₂·3H₂O in 100 mL of H₂O:DMF:EtOH. The Cu-BTC was obtained after adding 0.5 mL Et₃N to the solution of trimesic acid and Cu(NO₃)₂·3H₂O and stirring for 24 h at room temperature. The as-fabricated MOF was filtered and washed by the above-mentioned mixed solvent. Finally, the Cu-BTC was dried at 70 °C for 24 h [29].

Physical Characterization of the Cu(II)-BTC and Drug Loading Determination

The sample was characterized by

thermogravimetry (TG; TGA 7, NETZSCH Iris 209 F1, 10°C/ min, N₂ gas purge 20 mL.min⁻¹). The amount of drug loading determined by Thermal Gravimetric. In the this analysis, levothyroxine desorbs after decomposing of MOF, which is detected as a temperature-dependent weight decrease.

Surface Characterization

Scanning electron microscopy (FESEM-KYKY-EM3200) was utilized to characterize the porous layers. The surface roughness and topography of Cu(II)-BTC samples have been analyzed using atomic force microscopy (NanosurfMobile S scanning probe–optical microscope, Switzerland). Analysis of AFM images was done by NanosurfMobile S software. All scans were of an 8 μm*8 μm area.

Drug Loading

Drug loading was achieved at 37°C. The solubility of levothyroxine (poorly soluble in water) performed in non-aqueous solution. Instead, loading of the mesoporous Cu(II)-BTC was done in DMSO solution, since levothyroxine completely dissolves in DMSO. The mesoporous Cu(II)-BTC was immersed in levothyroxine solution in DMSO (10 mg mL⁻¹) at ambient conditions for 16 h, which was occasionally stirred during the loading. The MOF loaded by drug, washed quickly with DMSO to remove drugs were loosely attached on the surface of the nanoparticles.

A loading time of MOF was performed 16 h. The sample was dried in vacuum conditions at 60 °C and DMSO desorption was monitored daily with before each TG measurement [14,15].

No further DMSO desorption could be fined by TG measurement after 5 days of drying. The

quantification of the loaded drug was performed 2 min after the loading. Common advantages of this method are follow: the loading can be carried out at ambient conditions and the loaded drug is not exposed to a harsh chemical environment [30-31]. However, controlling the drug fraction of the particles or layers is more complicated, and additional surface washing may be necessary. It should be noted, that different dissolution rates between adherent drug molecules on the particle surface than those of the loaded ones may lead to inaccurate results. However, controlled washing of the loaded particles can be a challenging process, particularly when dealing with drugs that have low solubility [14-15]. Therefore it seems control on the loading procedure is more straightforward rather than washing processes [32]. Fig. 1. showed drug loading schematically into the Cu-BTC (MOF).

Determination of Levothyroxine Using UV Spectrophotometry

Release experiments were carried out in 10 mM phosphate buffer solution at (pH 7.4, 37 °C) in the sink condition using orbital shaking (75–100 rpm). The levothyroxine concentration in samples was detected by utilized UV spectrophotometry at the drug λ_{max} at 225 nm.

RESULTS AND DISCUSSION

FTIR studies

Porous Cu(II)-BTC was synthesized by reacting copper nitrate with trimesic acid as an organic linker in H₂O:DMF:EtOH. The FT-IR of the Cu-BTC were produced in the range of 400-4000 cm⁻¹ (Fig. 2). The band at 490 cm⁻¹ can be attributed to the Cu-O stretching vibrations. A band at 730 cm⁻¹ is related to the ν(C-H) vibrations. Two strong bands at 1376 cm⁻¹ and 1450 cm⁻¹ are ascribed to

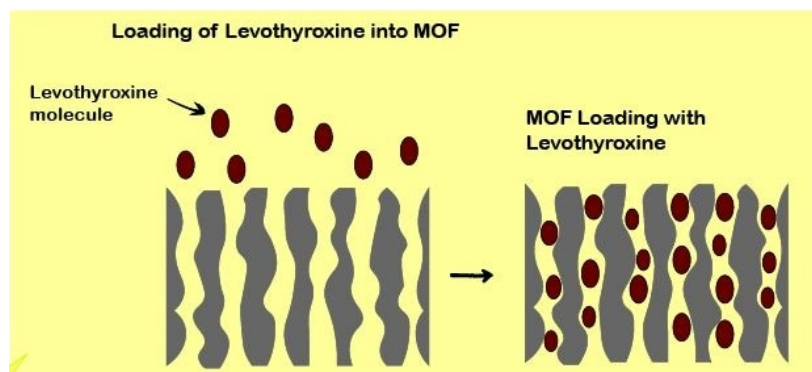


Fig. 1. The Schematic figure of loading of levothyroxine into MOF

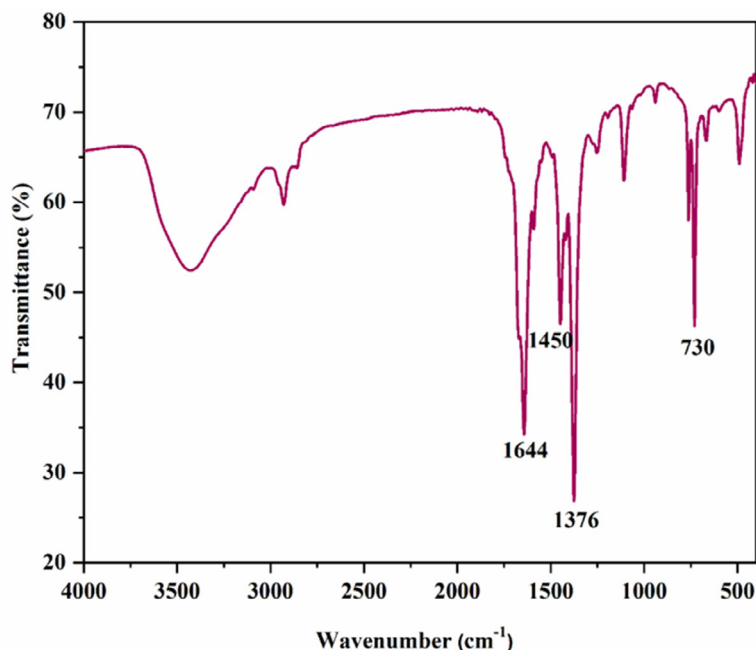


Fig. 2. FT-IR spectra of Cu-BTC.

the symmetric stretching vibrations of carboxylate groups. The $\nu(\text{COO}^-)$ asymmetric stretching vibrations band appears at 1644 cm^{-1} [33-34].

The PXRD pattern of the as-prepared Cu(II)-BTC displays diffraction peaks consistent with the simulated pattern, indicating that the Cu(II)-BTC is a pure product. The characteristic diffraction peaks of this compound are revealed at $2\theta = 6.55^\circ$ (200), 9.33° (220), 11.43° (222), 13.23° (400), 14.89° (331), 16.31° (422), 17.23° (551), and 18.85° (440) as shown in Fig. 3 [35]. The Debye-Scherrer equation, $D = K\lambda/\beta\cos\theta$, was utilized to detect the grain size (D) of the Cu-BTC, where D is the nanoparticles crystalline size, K is the Scherrer constant, λ denotes the wavelength of X-ray, and β represents the FWHM (full width at half maximum). The crystalline size of Cu-BTC nanoparticles are about 258-270 nm [36, 37].

The hydrophilicity of the as-synthesized Cu-MOFs was revealed by evaluating the water contact angles (WCA) analysis (Fig. 4). The Cu-MOFs exhibited proper hydrophilicity nature with a WCA of 36.2° .

Drug Loading Capacity

Quantification of drug load was done 5 min after the loading and is expressed as Eq.1 [32, 38]. The initial evaluation of the drug loading

degree by the data of thermal gravimetric showed that drug molecules have been loaded of about 23.72%, which establishes the need for chemical analysis inaccurate drug loading determination. The total loaded drug was also determined by extracting Cu(II)-BTC loaded by levothyroxine, in DMSO (5 ml) for 8 h with magnetic stirring, after which the samples analyzed by the UV absorption spectrophotometry indicated drug loads of about 20.14%. The total loaded drug was also detected by dissolved Cu(II)-BTC in H_2SO_4 solution (1 M) for 12 h; then the sample was analyzed by UV absorption spectrophotometry, which indicated that the drug has been loaded of about 21%. The average loaded drug was 21.62% (Table 2).

$$m_{\text{drug}} / (m_{\text{drug}} + m_{\text{particle}}) \times 100\% \quad (1)$$

SEM and AFM Studies

The morphology of Cu(II)-BTC was studied by SEM analysis (Fig. 5). As can be seen, distinct microcrystals with octahedral structures were seen for this Cu(II)-BTC. Primary endeavors within the ponders of mesoporous materials as medicate conveyance vehicles have been centered on their remarkable potential for controlled and localized drug delivery [37-39]. The property of mesoporous materials for the development of the

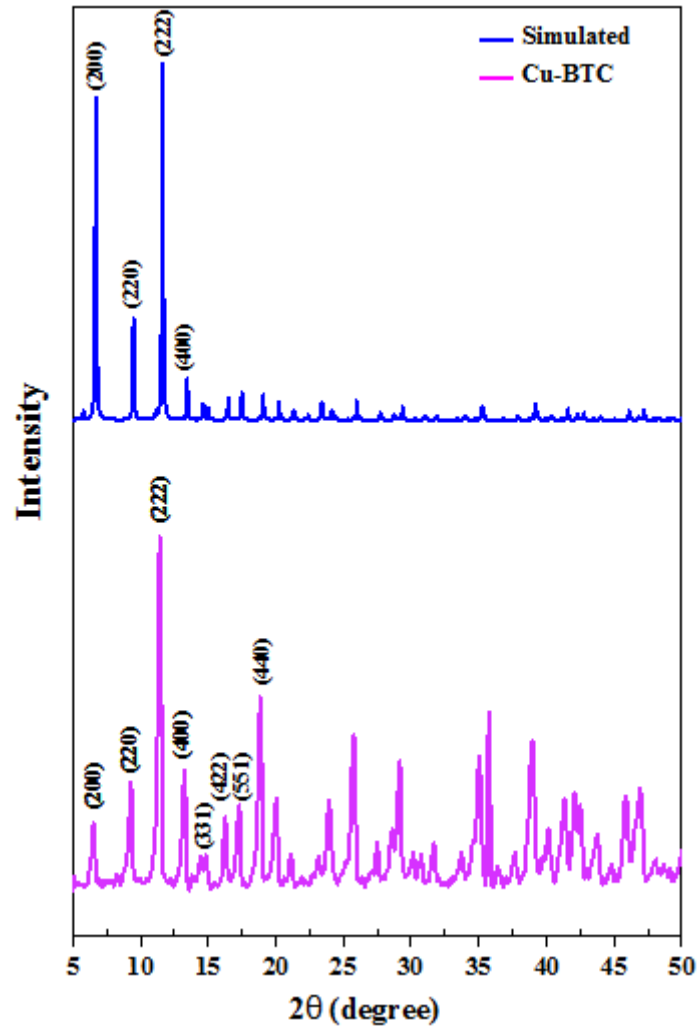


Fig. 3. XRD pattern of Cu-BTC

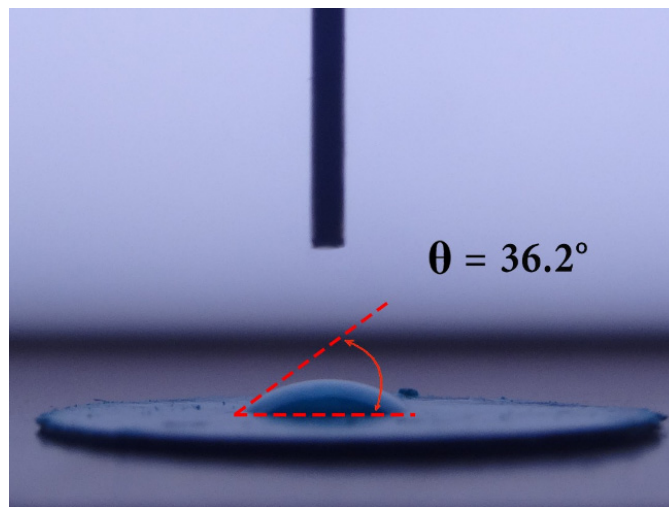


Fig. 4. Water contact angle of Cu-BTC

Table 2. Extent of drug loading (% w/w) determined from Cu(II)-BTC after drug loading utilizing different methods

Method	TGA	H2SO4	DMSO	Average drug load
Drug load	23.72%	21%	20.14%	21.62%

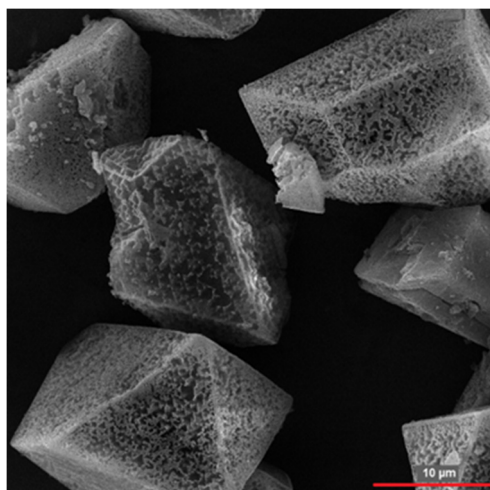


Fig. 5. SEM image of Cu-BTC.

permeability of large, hydrophilic drug substances has also been discovered in combination with classical permeation enhancers. Moreover, mesoporous materials provide a potential method to increase the solubility of the poorly soluble drug via effects on surface area or crystallinity [36]. AFM images showed the topographical characteristics changes among MOF before and after the loading of levothyroxine (Fig. 6). Area statistical rms roughness values for Cu(II)-BTC before loading (10.005 nm) were more than Cu(II)-BTC after loading (1.705 nm). Cu-BTC before loading was 8.295 nm rougher and more porous compared with Cu-BTC after loading. After drug loading, porosity was diminished because the pores were occupied by drug molecules. The results of the SEM and AFM analyses were consistent, demonstrating the mesoporous property of Cu(II)-BTC (Table 3).

Drug Release Evaluation and release kinetics calculation

During the loading process, levothyroxine molecules were adsorbed inside the mesoporous Cu-BTC. This action reduced the concentration of levothyroxine molecules in the solution, which reduced the absorption intensity of the solution spectra according to the Beer-Lambert law:

$$A = \alpha lc \quad (2)$$

Where A is absorbance, α is the absorption coefficient of the absorber, l is the path length of light, and c is the concentration of the absorber. The Beer-Lambert law is a well-established principle in analytical chemistry that relates the absorbance of a substance to its concentration, the path length of light through the substance, and the absorption coefficient of the substance. By using this law to analyze the absorption spectra. The release rate of the loaded levothyroxine at pH 7.4 was considered [16, 18, 26].

The initial rapid increase in absorption intensity indicated a burst release of levothyroxine at the beginning of the release process. The burst release pattern was due to the physically and chemically trapped drug molecules [20, 26]. According to levothyroxine's P_i in the upper pHs, the interaction between drug and the surface charges of Cu(II)-BTC is less effective, so the release of levothyroxine molecules in physiological pH is more and depends on loading condition such as drug concentration, kind of solvent and loading time. In pH 7.4, the amount of levothyroxine was showed $12.5 \mu\text{g mL}^{-1}$ in the 7 days. These drug doses could be applied for thyroid patients.

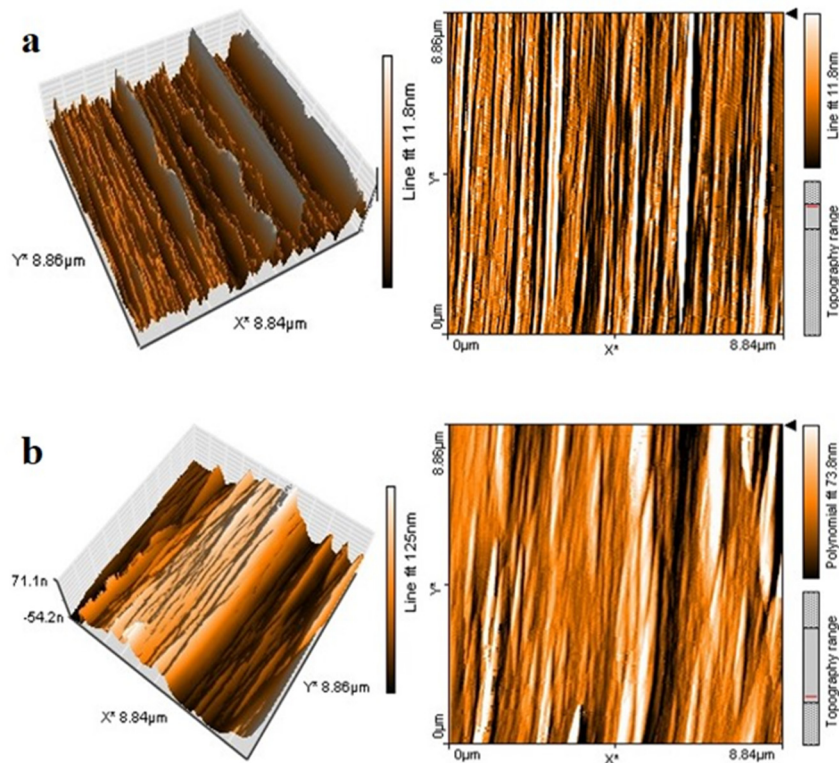


Fig. 6. AFM Topographical Characteristics Surface (a) Cu(II)-BTC before and (b) after Drug Loading.

Table 3. Area Statistical rms Roughness Values

MOF	Roughness parameters (nm)*		
	S _a **	S _q	S _y
MOF (before loading)	10.005	13.203	118.62
MOF(after loading)	1.705	2.949	30.366

Note: S_a, arithmetical mean height; S_q, root mean square height; S_y, peak-valley height.

These data demonstrated that, in principle, a controlled release from Cu(II)-BTC loaded with levothyroxine, was possible and a constant release was achieved for 7 days as it shown in Fig. 7. The burst release of levothyroxine was showed the quick adsorption of levothyroxine at the early stage of the drug loading process. This result of levothyroxine loading was compatible with the loading capacity experiment, in which the Cu(II)-BTC adsorbed the amount of levothyroxine molecules [16]. Furthermore, the Cu(II)-BTC showed initial burst release, and its release rate has been constant after about 7 days. The structure of pores had a crucial role in the loading and releasing of molecules. Through the drug loading process, the levothyroxine molecules distributed

into the Cu(II)-BTC pores at a higher rate than through and the diffusion rate reduced as the pores were occupied and the diffusion kinetics showed a pattern like to that of the loading, but in the conflicting direction [30-31, 38].

A handful of approaches can be utilized to look at dissolution profiles, for example, investigation of difference, model-free and model-dependent methodologies. In this dissolution study, model-dependent methodologies utilized for correlation of disintegration profiles. In model-dependent methodologies, discharge information were well suited

to five dynamic models including the zero-order (Eq. 3), first-order (Eq. 4), Higuchi grid (Eq.

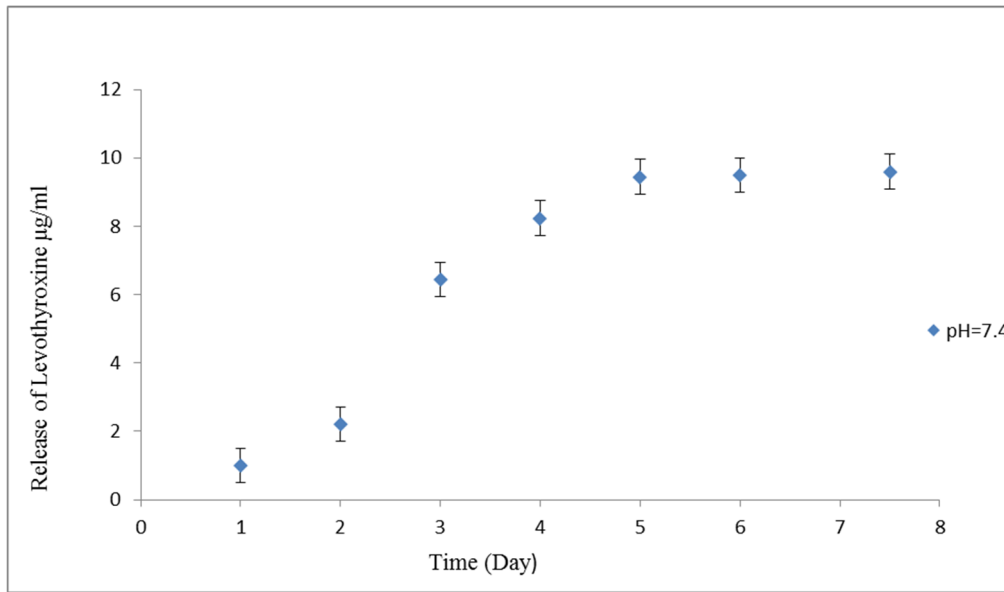


Fig. 7. Profiles Release of Levothyroxine from Cu(II)-BTC measured in phosphate buffer pH= 7.4, 37 °C (n = 3, mean ± sd) with UV assay.

5), and Peppas–Korsmeyer (Eq. 6), and discharge conditions, so as to find the best fit condition. Zero-order (Eq. 3) data is plotted as cumulative percentage drug released versus time.

$$C=K_0 t \quad (3)$$

The first equation that mentioned, known as the zero-order rate constant, relates the concentration of the drug to the time it takes to release it. The second equation, the first order equation, involves plotting the logarithm of the cumulative percentage of drug released against time [14,16].

$$\text{Log } C = \text{Log } C_0 - Kt/2.303 \quad (4)$$

Where C_0 is the initial concentration of the drug, K is the first-order rate constant, and t is the time.

$$Q = Kt^{1/2} \quad (5)$$

As per Higuchi's (Eq. 5) data is plotted as cumulative percentage drug released versus the square root of time. Where K is the constant of the system, and t is the time [14,16].

It's fascinating how the mechanism of drug release can be evaluated by plotting the percentage of drug released versus log time according to the Korsmeyer-Peppas equation. The exponent n ,

which indicates the mechanism of drug release, is calculated through the slope of the straight line. It's interesting to note that researchers used the n value to characterize different release mechanisms, concluding that values for a slab of $n < 0.5$ indicate Fick diffusion, while higher values of n between 0.5 and 1.0, or $n > 1.0$, indicate mass transfer following a non-Fickian model [14,16,23].

$$Mt/M_\infty = Ktn \quad (6)$$

The resulting release kinetics from the Cu(II)-BTC closely follows a first-order release profile with minimal burst effect. (Table 4.).

The main advantage of Cu(II)-BTC cover other nanocontainers, e.g., nanotubes, etc. is its ability to degrade in aqueous solutions. Moreover, they are relatively easy to prepare over a wide range of particle sizes [39]. Generally, biodegradability [40-41], biocompatibility [42], non-toxicity [4], and non-immunogenicity [43-44] of Cu(II)-BTC have made them widely used drug carriers for drug delivery.

These data have been showed the stable and constant levothyroxine dose for 7 days because Cu(II)-BTC loaded with levothyroxine has a constant controlled release. In general, levothyroxine therapy should be instituted at full replacement doses as soon as possible. Delays in diagnosis and therapy institution may have

Table 4. The R² values from in vitro release kinetics

Material	Zero order	First order	Higuchi	Krosmeier–Peppas Model	
				R	n
Cu-BTC	0.9029.922±0.0024	1	0.99290.922±0.0014	0.9468±0.0031	0.425±0.0034

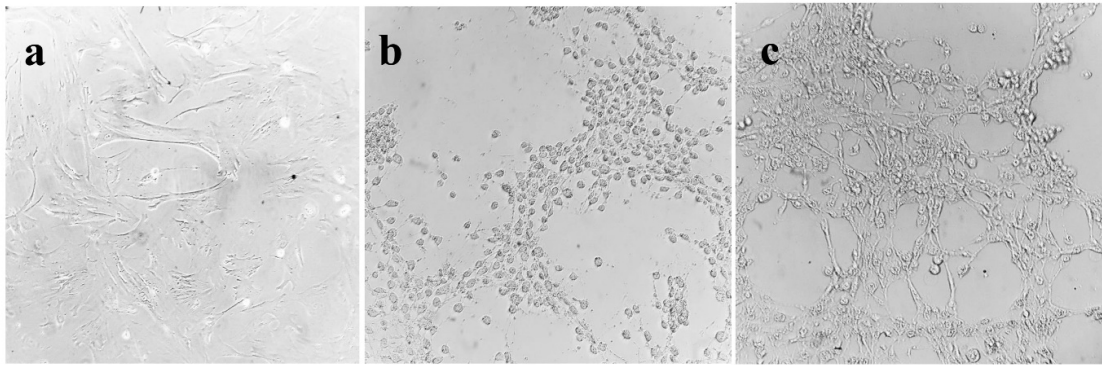
R² determination coefficient

Fig. 8. Inverted microscopic observation for a survey of cytotoxicity of drugs in WJMSCs for after 24 h a) The control cells b) WJMSCs were subjected to treatment with a concentration of 10 μ M levothyroxine. c) WJMSCs were ministered with a dose of 10 μ M Cu-BTC loaded with levothyroxine. 20X

deleterious effects on the child's intellectual and physical growth and development. .

MOFs seem to have some really unique properties that make them ideal for drug encapsulation, such as their intrinsic biodegradability due to relatively labile metal-ligand bonds and versatile functionality for postsynthetic grafting of drug molecules. It's really impressive how they have a higher drug-loading potential and improved controlled release kinetics when compared to conventional drug delivery systems like oral, buccal, rectal, intravenous, and intramuscular [10]. Several MOFs such as the microporous zinc imidazolate (ZIF-8), the zinc dicarboxylate (MOF-5) [22, 23], and the microporous copper trimesate HKUST-1, are recently studied MOF in the area of drug delivery. It's great that tuning of the pore size and adjustment of the functional groups can be done accordingly. It's no wonder that the Cu(II)-BTC was selected in this research due to its excellent biocompatibility and significant adsorption/drug-loading capacity [44-45].

Delivery of levothyroxine through oral and transdermal routes for subcutaneous lipid digestion has been reported [21, 22]. Recently, the potential of solid lipid nanoparticles (SLN) [23], the PEG-modified SLN [24], and chitosan [25] for levothyroxine delivery have been investigated.

The obtained results exhibited higher drug loading capacities and sustained drug release under physiological conditions for up to 7 days.

In vitro experiments

Effect of levothyroxine on morphological changes

The morphology of WJMSCs was investigated using an inverted microscope. Our results indicated that drugs had toxic effects in a dose dependent method. Also, levothyroxine showed more toxicity in WJMSCs than Cu(II)-BTC loaded by levothyroxine in similar concentrations. As showed in Fig 8, in the control group, the cell showed conventional properties of mesenchymal stem cells such as spindle shape with a high adhesion potential, uniformity nucleus, and high density while treated cells showed round and irregular appearance including chromatin condensation, vacuolated cytoplasm, and cellular shrinkage. These signs were more tangible in treated cells with levothyroxine than Cu(II)-BTC loaded by levothyroxine (Fig. 8).

Effect of levothyroxine on the cell viability

The effects of various concentrations of levothyroxine and Cu(II)-BTC loaded by levothyroxine on WJMSCs have been examined using the MTT test at 24 h. The obtained results

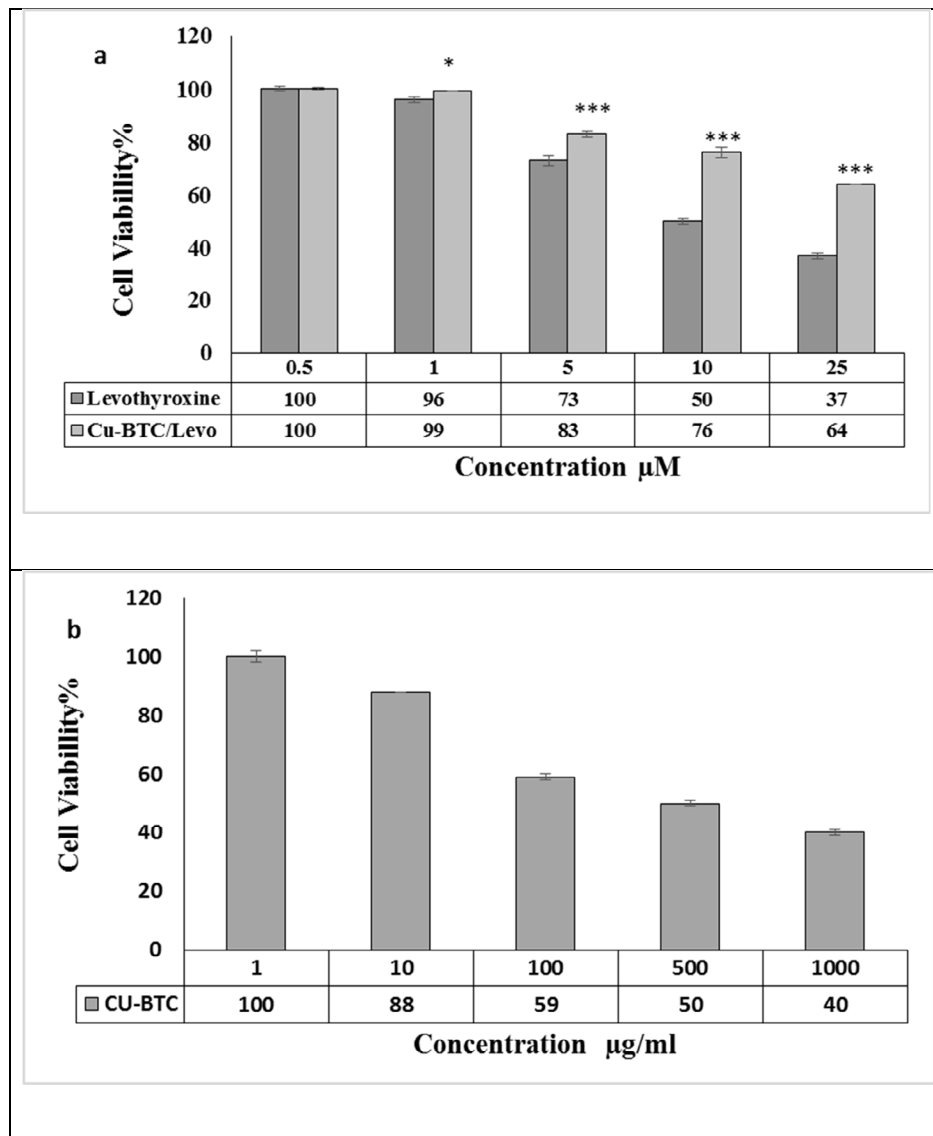


Fig. 9. Effect of drugs (levothyroxine, Cu-BTC loaded by levothyroxine, and Cu-BTC) on the cell viability and growth of WJMSCs by MTT assay a) WJMSCs treated with 25, 10, 5, 1, and 0.5 μM concentrations of levothyroxine and Cu-BTC loaded by levothyroxine after 24 h (b) WJMSCs treated with 1000, 500, 100, 10, and 1 $\mu\text{g/ml}$ concentrations of Cu-BTC after 24 h (*: $p < 0.05$ and values are mean ($n=3$)).

indicated that treated cells with various doses of drugs (levothyroxine, Cu(II)-BTC loaded by levothyroxine, and Cu(II)-BTC) significantly decrease the cell viability compared to control as a dose-dependent method. The drug toxicity effects were evaluated and our results indicated that the 25 μM concentration of levothyroxine was the most toxic one comparing to the other concentrations. The cell viability data indicated that levothyroxine was more toxic than Cu(II)-BTC loaded by

levothyroxine.

Also, the results indicated that the lowest concentration (0.5 μM) of levothyroxine and Cu(II)-BTC loaded by levothyroxine no toxic effect on the cell viability ($p < 0.001$) compared to the control group (Fig. 9).

Ansari et al.'s studies demonstrated that the tested sponges, including Cu-MOF@PDMS and Chitosan@Cu-MOF@PDMS scaffolds, demonstrated favorable levels of cell sticking,

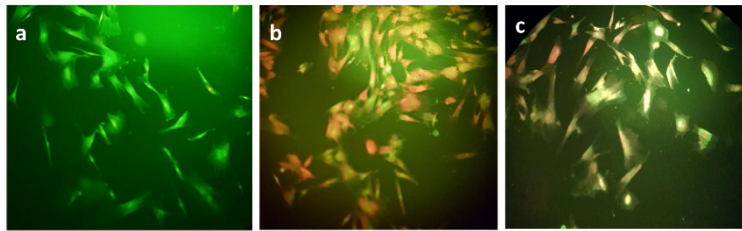


Fig. 10. Evaluation of the cell viability using Acridine orange/Ethidium bromide staining of WJMSCs by a fluorescent microscope a) The cells without any treatment as the control sample b) WJMSCs were subjected to treatment with a concentration of 10 μM levothyroxine. c) WJMSCs were ministered with a dose of 10 μM Cu-BTC loaded with levothyroxine. 40X.

expansion, and survival when compared to pure PDMS sponges. Furthermore, their findings confirmed the significant importance of Cu-MOF and chitosan in the nanocomposites for cell attachment and viability [46]. According to the studies conducted by researchers, it was concluded that encapsulating nanoparticles in a hydrogel matrix can reduce their toxicity and enhance cell proliferation. Researchers investigated the effects of nanoparticles on cell behavior when encapsulated within a hydrogel. Their findings discovered that the integration of nanoparticles into the hydrogel matrix led to a significant reduction in their toxicity. This encapsulation strategy effectively prevented direct contact between the nanoparticles and the cells, minimizing any potential adverse results. The controlled distribution of the nanoparticles from the hydrogel provided a sustained and localized delivery, which facilitated their interaction with the cells and stimulated cell growth. Overall, the research conducted by researchers supports the notion that encapsulating nanoparticles in a hydrogel matrix can enhance their biocompatibility and promote cell proliferation. This encapsulation technique has the potential to provide a safer and more effective approach for utilizing nanoparticles in various biomedical applications [47-48].

Additionally, in vitro biodegradation studies have indicated that hydrogels lacking certain nanoparticles, such as SiO_2 and ZrO_2 , exhibit greater instability compared to hydrogels incorporating nanoparticles. Moreover, the in vitro biocompatibility assessment of the tested hydrogels has revealed that cell viability and attachment are influenced by the presence of nanoparticles [49].

Staining of WJMSCs by Acridine orange

AO/EB is a doubling dye that greenish live cells, while oranges apoptotic cells. In WJMSCs treated with the 10 μM concentration of levothyroxine,

more apoptotic cells were found as compared to the WJMSCs treated with the 10 μM concentration of Cu(II)-BTC loaded by levothyroxine group and control. The control cells were dens, green, and without shrinkage indicating, their viability (Fig. 10).

CONCLUSION

It is imperative to the health of ~13 million thyroid patients in the United States that levothyroxine sodium products perform reliably and predictably.

levothyroxine may be administered to infants and children who cannot swallow intact tablets by crushing the tablet, so an implant of Cu(II)-BTC loaded by levothyroxine may be an attractive carrier that may be preferred for the sustained delivery of therapeutic agents. Thus, Cu(II)-BTC is expected to load and release a more considerable amount of drugs than non-porous thin film. The results of the SEM and AFM analysis were consistent and demonstrating the mesoporous property of Cu(II)-BTC before loading was slightly rougher (more porous) than Cu(II)-BTC after drug loading porosity was diminished because the pores occupy by the drug. Results of UV absorption demonstrated that the dose levothyroxine is constant in about 7 days. According to the obtained results of cell culture, loading of the levothyroxine into the Cu-BTC can be considered as a proper method for delivery of this drug in treatments applications.

ACKNOWLEDGMENT

The authors gratefully acknowledge financial support (Grant No.: SCU.SC98.31316) from the Shahid Chamran University of Ahvaz.

CONFLICT OF INTEREST

The authors declare no conflict of interest.

REFERENCES

- Ju, J., Gu, Z., Liu, X., Zhang, S., Peng, X., & Kuang, T. (2020). Fabrication of bimodal open-porous poly (butylene succinate)/cellulose nanocrystals composite scaffolds for tissue engineering application. *Int. J. Biol. Macromol.*, 147, 1164-1173. <https://doi.org/10.1016/j.ijbiomac.2019.10.085>
- Yao, C. H., Chen, K. Y., Cheng, M. H., Chen, Y. S., & Huang, C. H. (2020). Effect of genipin crosslinked chitosan scaffolds containing SDF-1 on wound healing in a rat model. *Mater. Sci. Eng. C*, 109, 110368. <https://doi.org/10.1016/j.msec.2019.110368>
- Kim, C., Kim, H., Park, H., & Lee, K. Y. (2019). Controlling the porous structure of alginate ferrogel for anticancer drug delivery under magnetic stimulation. *Carbohydr. Polym.*, 223, 115045. <https://doi.org/10.1016/j.carbpol.2019.115045>
- Lin, W.; Cui, Y.; Yang, Y.; Hu, Q.; Qian, G. (2018) A biocompatible metal-organic framework as a pH and temperature dual-responsive drug carrier, *Dalton Trans.*, 47, 15882-15887. <https://doi.org/10.1039/C8DT03202E>
- Liu, W.; Liu, L.; Ji, G.; Li, D.; Zhang, Y.; Ma, J.; Du, Y. (2017) Composition Design and Structural Characterization of MOF-Derived Composites with Controllable Electromagnetic Properties, *ACS Sustain. Chem. Eng.*, 5, 7961-71. <https://doi.org/10.1021/acssuschemeng.7b01514>
- Lu, L.; Ma, M.; Gao, C.; Li, H.; Li, L.; Dong, F.; Xiong, Y. (2020) Metal Organic Framework@Polysilsesquioxane Core/Shell-Structured Nanopatform for Drug Delivery, *Pharmaceutics*, 12, 98-113. <https://doi.org/10.3390/pharmaceutics12020098>
- Orellana-Tavra, C.; Köppen, M.; Li, A.; Stock, N.; Fairen-Jimenez, D. (2020) Biocompatible, Crystalline, and Amorphous Bismuth-Based Metal-Organic Frameworks for Drug Delivery, *ACS Appl. Mater. Interfaces*, 12, 5633-41. <https://doi.org/10.1021/acsnano.9b21692>
- Liu, W.; Zhong, Y.; Wang, X.; Zhuang, C.; Chen, J.; Liu, D.; Xiao, W.; Pan, Y.; Huang, J.; Liu, J. (2020) A porous Cu(II)-based metal-organic framework carrier for pH-controlled anticancer drug delivery, *Inorg. Chem. Commun.*, 111, 107675-107689. <https://doi.org/10.1016/j.inoche.2019.107675>
- Ricco, R.; Liang, S.; Gassensmith, J.J.; Caruso, F.; Doonan, F.; Falcaro, P. (2018) Metal–Organic Frameworks for Cell and Virus Biology: A Perspective, *ACS Nano*, 12, 13-23. <https://doi.org/10.1021/acsnano.7b08056>
- Simon-Yarza, T.; Mielcarek, A.; Couvreur, P.; Serre, C. (2018) Nanoparticles of Metal-Organic Frameworks: On the Road to In Vivo Efficacy in Biomedicine, *Adv. Mater.*, 1707365-1707380. <https://doi.org/10.1002/adma.201707365>
- Davis, M. E., Chen, Z., & Shin, D. M. (2010). Nanoparticle therapeutics: an emerging treatment modality for cancer. *J. Nanosci. Nanotechnol.: A collection of reviews from nature journals* (pp. 239-250). https://doi.org/10.1142/9789814287005_0025
- Dyson, P. J., & Sava, G. (2006). Metal-based antitumour drugs in the post genomic era. *Dalton Trans.*, 16, 1929-1933. <https://doi.org/10.1039/b601840h>
- Huxford, R. C., Della Rocca, J., & Lin, W. (2010). Metal-organic frameworks as potential drug carriers. *Curr Opin Chem Biol*, 14(2), 262-268. <https://doi.org/10.1016/j.cbpa.2009.12.012>
- Anglin, E. J., Schwartz, M. P., Ng, V. P., Perelman, L. A., & Sailor, M. J. (2004). Engineering the chemistry and nanostructure of porous silicon Fabry-Pérot films for loading and release of a steroid. *Langmuir*, 20(25), 11264-11269. <https://doi.org/10.1021/la048105t>
- Salonen, J., Kaukonen, A. M., Hirvonen, J., & Lehto, V. P. (2008). Mesoporous silicon in drug delivery applications. *J. Pharm. Sci.*, 97(2), 632-653. <https://doi.org/10.1002/jps.20999>
- Kashanian, S., Rostami, E., Harding, F. J., McInnes, S. J., Al-Bataineh, S., & Voelcker, N. H. (2016). Controlled delivery of levothyroxine using porous silicon as a drug nanocontainer. *Aust. J. Chem.*, 69(2), 204-211. <https://doi.org/10.1071/CH15315>
- Epstein, P. M. (2012). Bone and the cAMP signaling pathway: emerging therapeutics. In *Bone-Metabolic Functions and Modulators*, 271-287. Springer, London. https://doi.org/10.1007/978-1-4471-2745-1_16
- Blakesley, V. A. (2005). Current methodology to assess bioequivalence of levothyroxine sodium products is inadequate. *AAPS J.*, 7(1), E42-E46. <https://doi.org/10.1208/aapsj070105>
- Mandel, S. J., Brent, G. A., & Larsen, P. R. (1993). Levothyroxine therapy in patients with thyroid disease. *Ann. Intern. Med.*, 119(6), 492-502. <https://doi.org/10.7326/0003-4819-119-6-199309150-00009>
- Colucci, P., Yue, C. S., Ducharme, M., & Benvenega, S. (2013). A review of the pharmacokinetics of levothyroxine for the treatment of hypothyroidism. *Eur. J. Endocrinol.*, 9(1), 40. <https://doi.org/10.17925/EE.2013.09.01.40>
- Padula, C., Pappani, A., & Santi, P. (2008). In vitro permeation of levothyroxine across the skin. *Int. J. Pharm.*, 349(1-2), 161-165. <https://doi.org/10.1016/j.ijpharm.2007.08.004>
- Azarbayjani, A. F., Venugopal, J. R., Ramakrishna, S., Lim, F. C., Chan, Y. W., & Chan, S. Y. (2010). Smart polymeric nanofibers for topical delivery of levothyroxine. *J. Pharm. Pharm. Sci.*, 13(3), 400-410. <https://doi.org/10.18433/J3TS3G>
- Rostami, E., Kashanian, S., & Azandaryani, A. H. (2014). Preparation of solid lipid nanoparticles as drug carriers for levothyroxine sodium with in vitro drug delivery kinetic characterization. *Mol. Biol. Rep.*, 41(5), 3521-3527. <https://doi.org/10.1007/s11033-014-3216-4>
- Kashanian, S., & Rostami, E. (2014). PEG-stearate coated solid lipid nanoparticles as levothyroxine carriers for oral administration. *J. Nanoparticle Res.*, 16(3), 2293. <https://doi.org/10.1007/s11051-014-2293-6>
- Rostami, E., Kashanian, S., & Askari, M. (2014). The effect of ultrasound wave on levothyroxine release from chitosan nanoparticles. In *Adv Mat Res.*, 829, 284-288. Trans Tech Publications Ltd. <https://doi.org/10.4028/www.scientific.net/AMR.829.284>
- Schall Jr, R. F., Fraser, A. S., Hansen, H. W., Kern, C. W., & Tenoso, H. J. (1978). A sensitive manual enzyme immunoassay for thyroxine. *Clin. Chem.*, 24(10), 1801-1804. <https://doi.org/10.1093/clinchem/24.10.1801>
- Xiao, J., Zhu, Y., Huddleston, S., Li, P., Xiao, B., Farha, O. K., & Ameer, G. A. (2018). Copper metal-organic framework nanoparticles stabilized with folic acid improve wound healing in diabetes. *ACS nano*, 12(2), 1023-1032. <https://doi.org/10.1021/acsnano.7b01850>
- Zhuang, Y., Zhang, S., Yang, K., Ren, L., & Dai, K. (2020).

- Antibacterial activity of copper-bearing 316L stainless steel for the prevention of implant-related infection. *J. Biomed. Mater. Res.*, 108(2), 484-495. <https://doi.org/10.1002/jbm.b.34405>
29. Loera-Serna, S., Oliver-Tolentino, M. A., de Lourdes López-Núñez, M., Santana-Cruz, A., Guzmán-Vargas, A., Cabrera-Sierra, R., & Flores, J. (2012). Electrochemical behavior of Cu₃ (BTC) 2. metal-organic framework: The effect of the method of synthesis. *J. Alloys Compd.*, 540, 113-120. <https://doi.org/10.1016/j.jallcom.2012.06.030>
 30. Batten, S. R., Champness, N. R., Chen, X. M., Garcia-Martinez, J., Kitagawa, S., Öhrström, L., ... & Reedijk, J. (2013). Terminology of Metal-Organic Frameworks and Coordination Polymers (IUPAC Provisional Recommendation). Research Triangle Park, NC.
 31. Horcajada, P., Serre, C., Maurin, G., Ramsahye, N. A., Balas, F., Vallet-Regi, M., ... & Férey, G. (2008). Flexible porous metal-organic frameworks for a controlled drug delivery. *J. Am. Chem. Soc.*, 130(21), 6774-6780. <https://doi.org/10.1021/ja710973k>
 32. James, S. L. (2003). Metal-organic frameworks. *Chem. Soc. Rev.*, 32(5), 276-288. <https://doi.org/10.1039/b200393g>
 33. Li, Y., Miao, J., Sun, X., Xiao, J., Li, Y., Wang, H., ... & Li, Z. (2016). Mechanochemical synthesis of Cu-BTC@ GO with enhanced water stability and toluene adsorption capacity. *Chem. Eng. J.*, 298, 191-197. <https://doi.org/10.1016/j.cej.2016.03.141>
 34. Hosseini, M. S., Zeinali, S., & Sheikhi, M. H. (2016). Fabrication of capacitive sensor based on Cu-BTC (MOF-199) nanoporous film for detection of ethanol and methanol vapors. *Sens. Actuators B Chem.*, 230, 9-16. <https://doi.org/10.1016/j.snb.2016.02.008>
 35. Salonen, J., Laitinen, L., Kaukonen, A. M., Tuura, J., Björkqvist, M., Heikkilä, T., ... & Lehto, V. P. (2005). Mesoporous silicon microparticles for oral drug delivery: loading and release of five model drugs. *J. controlled release*, 108(2-3), 362-374. <https://doi.org/10.1016/j.jconrel.2005.08.017>
 36. Y. Orooji, M. Ghanbari, O. Amiri and M. Salavati-Niasari, *J. Hazard. Mater.*, 2020, 389, 122079. <https://doi.org/10.1016/j.jhazmat.2020.122079>
 37. M. Karami, M. Ghanbari, H. A. Alshamsi, S. Rashki and M. Salavati-Niasari, *Inorg. Chem. Front.*, 2021, 8, 2442-2460. <https://doi.org/10.1039/D1QI00155H>
 38. Yan, W., Hsiao, V. K., Zheng, Y. B., Shariff, Y. M., Gao, T., & Huang, T. J. (2009). Towards nanoporous polymer thin film-based drug delivery systems. *Thin Solid Films*, 517(5), 1794-1798. <https://doi.org/10.1016/j.tsf.2008.09.080>
 39. Miller, S. R., Heurtaux, D., Baati, T., Horcajada, P., Grenèche, J. M., & Serre, C. (2010). Biodegradable therapeutic MOFs for the delivery of bioactive molecules. *ChemComm*, 46(25), 4526-4528. <https://doi.org/10.1039/c001181a>
 40. Cai, X., Xie, Z., Ding, B., Shao, S., Liang, S., Pang, M., & Lin, J. (2019). Monodispersed Copper (I)-Based Nano Metal-Organic Framework as a Biodegradable Drug Carrier with Enhanced Photodynamic Therapy Efficacy. *Adv. Sci. Lett.*, 6(15), 1900848. <https://doi.org/10.1002/advs.201900848>
 41. Gulcay, E., & Erucar, I. (2019). Biocompatible MOFs for Storage and Separation of O₂: A Molecular Simulation Study. *Ind. Eng. Chem. Res.*, 58(8), 3225-3237. <https://doi.org/10.1021/acs.iecr.8b04084>
 42. Lin, W., Cui, Y., Yang, Y., Hu, Q., & Qian, G. (2018). A biocompatible metal-organic framework as a pH and temperature dual-responsive drug carrier. *Dalton Trans.*, 47(44), 15882-15887. <https://doi.org/10.1039/C8DT03202E>
 43. Neisi, Z., Ansari-Asl, Z., Jafarinejad-Farsangi, S., Tarzi, M. E., Sedaghat, T., & Nobakht, V. (2019). Synthesis, characterization and biocompatibility of polypyrrole/Cu (II) metal-organic framework nanocomposites. *Colloids Surfaces B*, 178, 365-376. <https://doi.org/10.1016/j.colsurfb.2019.03.032>
 44. Gan, S., Tong, X., Zhang, Y., Wu, J., Hu, Y., & Yuan, A. (2019). Covalent Organic Framework-Supported Molecularly Dispersed Near-Infrared Dyes Boost Immunogenic Phototherapy against Tumors. *Adv. Funct. Mater.*, 29(46), 1902757 <https://doi.org/10.1002/adfm.201902757>
 45. Gautam, S., Singhal, J., Lee, H.K., Chae K.H., (2022). Drug delivery of paracetamol by metal-organic frameworks (HKUST-1): improvised synthesis and investigations. *Mater. Today Chem.*, 23(100647). <https://doi.org/10.1016/j.mtchem.2021.100647>
 46. Ansari-Asl, Z., Shahvali, Z., Sacourbaravi, R., Hoveizi, E., Darabpour, E., (2022). Cu (II) metal-organic framework@ Polydimethylsiloxane nanocomposite sponges coated by chitosan for antibacterial and tissue engineering applications. *Microporous and Mesoporous Materials.*, 336 111866. <https://doi.org/10.1016/j.micromeso.2022.111866>
 47. Ischakov, R., Adler-Abramovich, L., Buzhansky, L., Shekhter, T., Gazit, E., (2013). Peptide-based hydrogel nanoparticles as effective drug delivery agents. *Bioorganic & medicinal chemistry*. 21 3517-22. <https://doi.org/10.1016/j.bmc.2013.03.012>
 48. Zhao, H., Hao, S., Fu, Q., Zhang, X., Meng, L., Xu, F., Yang, J., (2022) Ultrafast fabrication of lignin-encapsulated silica nanoparticles reinforced conductive hydrogels with high elasticity and self-adhesion for strain sensors. *Chemistry of Materials.*, 34 5258-72. <https://doi.org/10.1021/acs.chemmater.2c00934>
 49. Ahmed, K., Hassan, MM., Kabir, MA., (2021) Handbook of Polymer and Ceramic Nanotechnology for Biomedical Applications. Springer., pp 1357-75. https://doi.org/10.1007/978-3-030-40513-7_83